frontiers in Earth Science

ORIGINAL RESEARCH
published: 02 March 2022
doi: 10.3389/feart.2021.774501

Geochemistry of Formation Water and Its Implications for Petroleum Source Rocks in the Fengcheng Formation, Mahu Depression, Xinjiang, China

Jian Wang[1,2,3], Lu Zhou[1,3], Jin Liu[2], Xinji Zhang[5], Xiaojing Luo[6], Rong Zhu[4], Yong Wu[1,3], Zhaoyan Ren[2] and Jeffrey Dick[7]**

[1]State Key Laboratory of Oil and Gas Reservoir Geology and Exploitation, Southwest Petroleum University, Chengdu, China, [2]Research Institute of Experiment and Detection, Xinjiang Oilfield Company PetroChina, Karamay, China, [3]School of Geosciences and Technology, Southwest Petroleum University, Chengdu, China, [4]Institute of Hydrology and Water Resource Engineering, Zhejiang University, Hangzhou, China, [5]Exploration and Development Research Institute, Xinjiang Oilfield Company PetroChina, Karamay, China, [6]Fengcheng Oilfield Operation Area, Xinjiang Oilfield Company Petrochina, Karamay, China, [7]School of Geosciences and Info-physics, Central South University, Changsha, China

OPEN ACCESS

Edited by:
Jingqiang Tan,
Central South University, China

Reviewed by:
Youliang Ji,
China University of Petroleum, China
Wu Kongyou,
China University of Petroleum, China

***Correspondence:**
Lu Zhou
Zhoulu9@126.com
Jeffrey Dick
jeff@chnosz.net

Specialty section:
This article was submitted to Economic Geology, a section of the journal Frontiers in Earth Science

Received: 12 September 2021
Accepted: 07 December 2021
Published: 02 March 2022

Citation:
Wang J, Zhou L, Liu J, Zhang X, Luo X, Zhu R, Wu Y, Ren Z and Dick J (2022) Geochemistry of Formation Water and Its Implications for Petroleum Source Rocks in the Fengcheng Formation, Mahu Depression, Xinjiang, China. Front. Earth Sci. 9:774501. doi: 10.3389/feart.2021.774501

Geochemical properties of formation water reflect the sedimentary environments and the sealing conditions of the formation, which are of great significance for oil and gas exploration. In this research, the formation waters in the deep Permian Fengcheng Formation in the Mahu Depression were studied by analysis of chemical composition, stable isotopes, and the homogenization temperatures and salinities of fluid inclusions. The results show that the formation water is $NaHCO_3$-type with high salinity, high HCO^{3-}, low concentrations of Ca^{2+} and Mg^{2+} and high pH. The overall sealing of the formation is well maintained. Na_2SO_4-type water was found in some places with poor preservation of oil and gas. The fluid geochemistry and alkaline mineral distribution in the strata, which are dominated by deep fine-grain mixed deposits, indicate that the main body of the Fengcheng Formation was deposited in an alkaline lake sedimentary environment. The isotopic signatures are characterized by high $\delta^{13}C$, negative $\delta^{18}O$, and light strontium and heavy boron isotopes in the strata near the deep fault zone, which indicate that the Fengcheng formation may have been affected by deep hydrothermal fluids. From the first member to the third member of the formation, the salinity first increases and then decreases. This low-high-low trend corresponds to the initial stage of alkaline lake development followed by strong alkali formation and a final stage of water retreat. The coincidence between the spatial distribution of alkaline minerals, high-salinity formation water and source rocks indicates that the alkaline lake environment can form high-quality source rocks with good petroleum generation capacity.

Keywords: geochemical characteristics, fengcheng formation, mahu depression, sealing conditions, formation water

INTRODUCTION

Formation water is a geological fluid that exchanges material and energy with surrounding rocks and preserves much information about original sedimentary water. In petroleum reservoirs, formation water coexists with oil and gas in different phases. Formation water consequently can record the processes of formation, migration, accumulation, preservation, and alteration of petroleum. In fact, the type, salinity and ionic composition of formation water have been widely used to elucidate the source of formation water, the dynamic environment of water, the strength of water-rock interaction, and in the exploration of oil and gas reservoirs (Garven, 1989; Zhang et al., 2021). In essence, the composition of formation water is the result of the alteration and mixing effect of flow processes as well as water-rock interactions that occur during sedimentation and burial (Jin et al., 2006). Previous studies on formation water in sedimentary basins have focused on the origin of formation water through flowing and mixing, the mechanism of formation water concentration and desalination, and the origin of ions in formation water in the process of water-rock interaction (Meng et al., 2018). The chemical characteristics, dynamic field characteristics, and significance to petroleum exploration have been widely documented (Si, 2019; Lou et al., 2006; Lou et al., 2005; Lou et al., 2009). In particular, formation water can provide information about the conditions of petroleum generation and preservation in alkaline sedimentary environments, such as the Mahu Depression, which is an area of intense exploration for petroleum resources.

The Mahu Depression, also known as the Mahu Sag, is located in the northwest margin of the Junggar Basin in Xinjiang, northwestern China. The depression is separated from Mount Zaire and Mount Haraalt by the Wuxia and Kebai fault zones in the west and is bounded by the Zhongguai uplift in the southwest, the Xiayan uplift, Dabasong uplift and Yingxi Depression in the southeast, and an uplift in the north (**Figure 1**). The deep sediments of the Permian Fengcheng Formation in the Mahu Depression are important petroleum source rocks and shale oil targets (Kuang et al., 2012; Wang M et al., 2018; Zhang Y et al., 2018). The Junggar Basin experienced six tectonic stages, i.e., Carboniferous fault-depression, Early Permian fault-depression, Middle Permian-Triassic foreland basin, Jurassic extensional fault-depression and compression-torsion basin, Cretaceous-Paleogene intracontinental depression, and Neogene-Quaternary intracontinental foreland basin. At the end of the Early Permian uplift, an unconformity developed at the top of Fengcheng Formation, and the tectonic regime changed from extension to compression (He et al., 2018).

The Fengcheng Formation contacts conformably or unconformably at a low angle with the Lower Jiamuhe

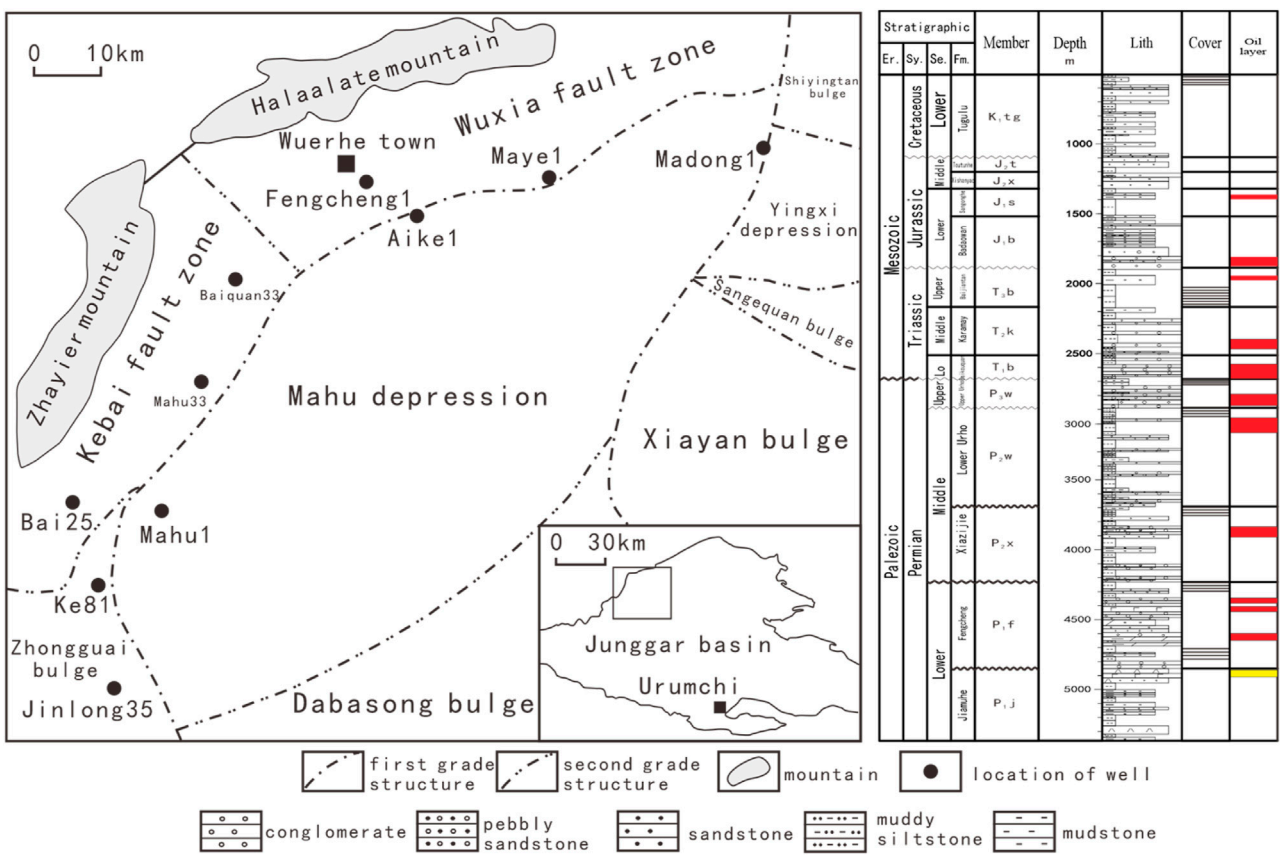

FIGURE 1 | Geological map of the Mahu Depression and sample locations.

TABLE 1 | Carbon, oxygen, strontium, and boron isotopic compositions of samples from the Permian Fengcheng Formation in the Mahu Depression. The paleosalinity index (*Z*) is defined in the text.

Well	Member	Depth/m	Lithology	$\delta^{13}C$ (‰)	$\delta^{18}O$ (‰)	$\delta^{11}B$ (‰)	$^{87}Sr/^{86}Sr$	Z
Feng 15	$P_1f_3^3$	2,999.99	argillaceous dolomite	2.366	−11.672		0.710019	126
Feng 15	$P_1f_2^1$	3,149.79	argillaceous dolomite	4.813	−7.020		0.706862	134
Feng 15	$P_1f_2^1$	3,229.6	dolomite	1.821	−8.608		0.710084	127
Feng 15	$P_1f_2^1$	3,464.3	argillaceous dolomite	5.091	−5.847		0.708226	135
Fengnan 1	$P_1f_3^2$	4,125.2	dolomitic mudstone	5.754	2.197		0.706612	140
Fengnan 1	$P_1f_2^1$	4,192.65	sedimentary tuff	5.532	−4.017		0.708006	137
Fengnan 1	$P_1f_2^2$	4,237.7	reedmergnerite			1.42		
Fengnan 1	$P_1f_2^2$	4,251.83	argillaceous dolomite	3.630	−5.781		0.706574	132
Fengnan 1	$P_1f_2^3$	4,327.4	reedmergnerite			2.13		
Fengnan 1	$P_1f_2^3$	4,338.0	argillaceous dolomite	2.163	−3.287		0.706349	130
Fengnan 1	$P_1f_2^3$	4,359.5	reedmergnerite			0.33		
Fengnan 2	$P_1f_2^1$	4,041.3	reedmergnerite			0.43		
Feng 5	$P_1f_2^1$	3,231.25	dolomite	4.503	−2.682		0.706741	135
Feng 5	$P_1f_1^1$	3,478.35	dolomite	4.605	−5.539		0.706710	134
Feng 26	$P_1f_3^2$	3,271.1	dolomite	3.145	−11.866		0.706676	128
Feng 26	$P_1f_3^2$	3,287	dolomite	5.307	−6.632		0.707273	135
Feng 8	$P_1f_3^3$	3,045.59	dolomite	5.114	−1.626		0.706732	137
Feng 8	$P_1f_2^1$	3,091.78	dolomite	5.124	−8.811		0.707211	133
Feng 8	$P_1f_2^2$	3,167.7	dolomite	2.492	−4.028		0.706358	130
Feng 8	$P_1f_2^3$	3,232.65	dolomite	3.998	−9.881		0.706313	131
Fengnan 7	$P_1f_2^2$	4,595.3	dolomitic mudstone	2.086	2.494		0.706999	133
Fengnan 7	$P_1f_2^2$	4,596.05	halite	2.318	1.350		0.706473	133
Fengnan 7	$P_1f_2^2$	4,597.35	halite	2.056	−0.835		0.707886	131
Xia 40	$P_1f_3^3$	4,582.7	sedimentary tuff	-1.542	−2.400		0.706429	123
Xia 40	$P_1f_2^1$	4,638	sedimentary tuff	-0.906	−9.158		0.705833	121
Xia 40	$P_1f_1^1$	4,826.4	tuff sandstone	0.352	−7.516		0.706500	124
Aike 1	$P_1f_1^2$	5,668.7	silty mudstone	2.138	−2.437		0.706325	130

Formation, and can be subdivided into Member I (P_1f^1), Member II (P_1f^2), and Member III (P_1f^3) in an ascending order. Member I (P_1f^1) is interbedded with gray mudstone, sandy conglomerate and sandstone, Member II (P_1f^2) is volcanic basalt, and Member III (P_1f^3) is gray sandstone, pebbly sandstone, mudstone and siltstone. At present, the influence of the sedimentary environment on the source rocks of the Fengcheng Formation is still uncertain: in particular, the evidence that the Fengcheng Formation can form high-quality source rocks in an alkaline sedimentary environment is not adequate (Yang et al., 2014; Xia et al., 2017). The lithology of the Fengcheng Formation is complex, showing mixed sedimentary characteristics, including dolomite, clastic rock and volcanic rock (Feng et al., 2011; Zhi et al., 2016). There are different concepts about the genesis of dolomite in alkaline lake sedimentation and hydrothermal activities (Zeng et al., 2002; Xian et al., 2013; Qin et al., 2016). The deep lacustrine sedimentary rocks of the Fengcheng Formation are rich in many types of evaporitic minerals, including sodium borosilicate, calcium carbonate, bischofite, rock salt, anhydrite, natural alkali and sodalite (Mello and Maxwell, 1990; Jiang et al., 2012; Wang X et al., 2018).

Whether the stratigraphic sealing of the Mahu Sag is intact and whether a considerable amount of sedimentary water is preserved in the formation are of great significance for reconstructing the sedimentary environment and for oil and gas exploration. In this paper, by collecting core and formation water samples from typical wells of the Fengcheng Formation, and analyzing the ionic and isotopic composition, fluid inclusion properties, and geochemical characteristics, the factors influencing the composition of formation water in the Mahu Sag are systematically studied. The sedimentary environments of source rocks in the Fengcheng Formation are integrated with large-scale geological characteristics.

SAMPLES

A total of 27 core samples were collected from 8 wells (i.e., Feng 15, Fengnan 1, Fengnan 5, Feng 26, Feng 8, Fengnan 7, Xia 40 and Aike 1), including members Feng 1, Feng 2 and Feng 3 (**Table 1**). The sample locations are mainly to the east and southeast of the town of Wuerhe (**Figure 1**). The carbon, oxygen, and strontium isotopes were analyzed for carbonate samples such as dolomite or argillaceous dolomite, while boron was analyzed from well-developed dolomite and layered tuff samples. The samples for fluid inclusion analysis were obtained from carbonate and evaporitic minerals, which have a linear or zonal distribution in dolomite fractures, and calcite fillings and sodium borosilicate minerals.

A large number of samples of formation water of the study area were collected from different horizons, including 6915 formation water samples obtained from different depths Formation. In total, the geochemistry of 6915 formation water samples was analyzed including 1,071 samples from the

Fengcheng Formation, 400 samples from other Permian formations, and 5,444 samples from formations of other geological ages (Carboniferous, Triassic, Jurassic, Cretaceous, Eocene, and Neogene). Measurements of hydraulic head are available for 626 piezometric wells in the study area (Jian et al., 2020).

METHODS

Thin sections for all samples were used for petrological identification using a Zeiss optical microscope. In order to accurately distinguish dolomite from calcite under the microscope, all thin sections were stained with alizarin red.

The most uniform part of the fresh surface of each sample was used for elemental and isotopic analyses. Fresh sample powder was obtained from an area with a diameter of about 1 cm by using micro-drilling to avoid the interference of impurities and carbonate texture differences on the subsequent analyses. The powder was then ground in an iron mortar and an agate mortar successively until the particle diameter was less than 200 mesh. The ground powder was used for elemental and stable isotope analyses.

Whole rock carbon and oxygen isotopic compositions were determined in the State Key Laboratory of Oil and Gas Resources and Exploration, China University of Petroleum (Beijing). The analysis was carried out by using the McCrea orthophosphoric acid method. The sample was reacted with anhydrous phosphoric acid in a water bath at 25°C for 24 h. Isotope abundances were analyzed on a Finnigan-MAT 252 gas isotope mass spectrometer with analysis error of ±0.1‰ and reported relative to the VPDB standard. The working standard sample for the carbon and oxygen isotopes was calcium carbonate reference material (GBW04405 from PetroChina Exploration and Development Research Institute).

Boron isotopes were measured by ICP-MS on a PGS-IIc0006 mass spectrometer in the Laboratory of Chengdu Univerisity of Technology (Chengdu, China).

Homogenization and freezing point temperature measurements of fluid inclusions were carried out in Zhejiang University, Hangzhou, China. The instrument used was LINKAM THMS600 cold and hot table no. 7035. The temperature and humidity in the laboratory were 25°C and 40%, respectively, and standard method EJ/T 1105-1999 was used for determination of mineral fluid inclusion temperature.

Formation water analyses were performed in the Research Institute of Experiment and Detection, Xinjiang Oilfield Company PetroChina, according to standard SY/T 5523-2016 (oilfield water analysis method). SO_4^{2-} analysis was performed with a 7230G visible light spectrophotometer from Shanghai Precision Scientific Instrument Co., Ltd., with an analysis wavelength of 420 nm and measurement accuracy of ±1 nm. CO_3^{2-}, HCO^{3-} and pH were analyzed by chemical titration using a magnetic PHS-3E pH meter with resolution of 0.01 pH unit. Ca^{2+} and Mg^{2+} were analyzed by chemical titration. The sum of Na^+ and K^+ was calculated by chemical charge balance.

RESULTS

Carbon and Oxygen Isotopes

The $\delta^{13}C$ (PDB) values of carbonate in the Fengcheng Formation range from −1.5 to 5.8‰, with an average value of 3.1‰ (**Table 1**). Previously, it was found that the $\delta^{13}C$ (PDB) values of Carboniferous rocks range from −17.9 to 2.3‰, with an average of −7.6‰ (Cao et al., 2007). Compared with the Carboniferous, the Fengcheng Formation is enriched in heavier carbon, indicating that it is significantly affected by deep hydrothermal fluids (Zhi et al., 2016). The carbon in the Carboniferous carbonates is isotopically lighter, reflecting a strong influence by atmospheric water (Cao et al., 2007) (**Figure 2**). We used formula $Z = 2.048 \times (\delta^{13}C + 50) + 0.498 \times (\delta^{18}O + 50)$ (Keith and Weber, 1964) to calculate the paleosalinity index (Z-value) for fluid inclusions in calcite veins in the Fengcheng Formation. It is generally believed that $Z > 120$ is characteristic of marine carbonate and $Z < 120$ is characteristic of freshwater carbonate (Keith and Weber, 1964). The paleosalinity indexes for the Fengcheng Formation and Carboniferous are very different (**Table 1**). The Z-values of the Fengcheng Formation are all greater than 120, which indicates that the carbonate cements were formed in a high salinity marine sedimentary environment and were weakly affected by atmospheric water infiltration. The paleosalinity is highest in the second member of the Fengcheng Formation. The Z-value for Carboniferous carbonates is generally less than 120, which indicates that carbonate cements were formed in a freshwater diagenetic environment.

In general, the $\delta^{13}C$ and $\delta^{18}O$ values increase as salinity increases, whereas $\delta^{18}O$ decreases with increasing temperature; in addition, during diagenesis, fresh water leaching and biodegradation can result in lower $\delta^{13}C$ and $\delta^{18}O$ (Liu et al., 2006). Because the carbon isotope fractionation effect is relatively insensitive to temperature, the $\delta^{13}C$ value of carbonate cements can be used as an indicator of the source of carbon in the fluids. During diagenesis, infiltration of atmospheric water along unconformities and phreatic seepage zones dissolves the underlying carbonates or replaces the carbonates formed in the early stage. In this process, a negative value of $\delta^{18}O$ will be observed in the carbonate cement or filling, while the $\delta^{13}C$ values can be traced to their original carbon source. Therefore, the lower values of $\delta^{18}O$ and $\delta^{13}C$ of secondary carbonates than those of primary minerals indicate that atmospheric fresh water was involved in diagenesis.

The oxygen isotopes are more sensitive to alteration processes than carbon isotopes and are easily affected by both the "age effect" and "diagenesis effect". The $\delta^{18}O$ is also affected by temperature. With the increase of burial depth and temperature, the isotopic fractionation of oxygen is more extensive, and the $\delta^{18}O$ of calcite cement becomes more negative. The $\delta^{18}O$ values of the Fengcheng Formation range from -11.866 to 2.494‰ (**Table 1**). The low $\delta^{18}O$ value indicates that carbonate was formed in hydrothermal conditions (Zeng et al., 2002). At the same time, isotopic exchange between diagenetic fluid and atmospheric gases or fresh water cannot be ruled out, which would result in lower $\delta^{18}O$ values. Although older carbonates have more time to exchange with atmosphere

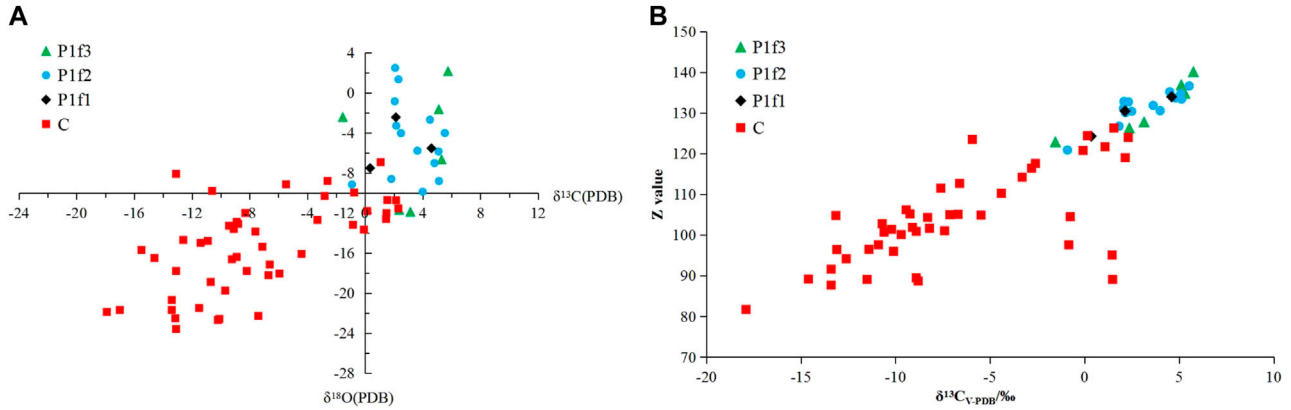

FIGURE 2 | Carbon and oxygen isotope relationship **(A)** and Z-value ~ carbon isotopic relationship **(B)** for the Permian Fengcheng Formation and Carboniferous strata in the Mahu Depression. Abbreviations: P_1f_1, P_1f_2, P_{13}—Members I, II, and III of the Fengcheng Formation; C–Carboniferous. Data for Carboniferous rocks are from Cao et al. (2007).

and free water, there is no significant difference in the carbon and oxygen isotope values among the first, second and third members.

Strontium Isotopes

The two major reservoirs for strontium in rocks are crust and mantle. The strontium input from crust *via* continental weathering has a higher ratio of $^{87}Sr/^{86}Sr$, with an average value of 0.7119 (Palmer and Edmond, 1989). However, mantle-derived strontium, which is mainly derived from hydrothermal fluids at mid-ocean ridges, has a lower $^{87}Sr/^{86}Sr$, with an average value of 0.7035 (Gieskes et al., 1986; Palmer and Edmond, 1989; Liu et al., 2017). Therefore, the $^{87}Sr/^{86}Sr$ can be used to trace the characteristics of fluids.

Table 1 shows that the $^{87}Sr/^{86}Sr$ of the Fengcheng Formation ranges from 0.705833 to 0.710084, which is between the values for crust and mantle, suggesting that the fluids might be affected by a combination of mantle and crustal sources. However, most samples have values of $^{87}Sr/^{86}Sr$ close to that of the mantle, which indicates that the fluid might have a deep hydrothermal fluid origin.

Boron Geochemistry

The Fengcheng Formation was deposited in a volcanic-alkaline lake evaporitic environment. Because boron is a reactive element, which often forms volatile, fusible and soluble complexes, it can migrate and accumulate during magmatism and is related to volcanic and hydrothermal activities (Wei et al., 2021). The abundance of boron in the upper crust is very low, so it is difficult to form boron-rich minerals. In tectonically active areas, boron is easily leached by hot water and migrates. Therefore, the source of boron-rich minerals is often related to hot springs or volcanism (Chang et al., 2016). Boron isotope composition (δ11B value) is usually determined by sample extraction, boron separation and purification, and computer determination. Boron extraction, separation and purification include:1. Decomposition of solid samples: Prior to the determination of B content and δ11B value, the solid sample needs to be dissolved into liquid, and after the decomposition of the sample, boron can be separated and extracted. According to the physical and chemical characteristics of the solid sample and the components to be extracted, different dissolution methods can be used:1) Acid dissolution; 2) hot water leaching method; 3) ashing method; 4) High temperature hydrolysis; 5) high temperature alkali fusion method.2. Boron separation and purification: after the solid liquefaction treatment, the matrix is very complex, and it must be partially purified to separate boron from other elements. The common methods for separation and purification of boron include:1) methyl borate distillation; 2) Chromatographic separation; 3) gas phase separation; 4) High temperature hydrolysis technology; 5) Ion exchange method and microsublimation technology.3. Determination of boron concentration: In nature, the content of B in various plastids is usually small, so boron is an element that is difficult to be accurately analyzed. Boron samples with different substance types and occurrence environments also have different requirements for analysis and testing methods. Common trace boron analysis methods include:1) Inductively coupled plasma emission spectrometry (ICP-OES); 2) Inductively coupled plasma mass spectrometry (ICP-MS); 3) spectrophotometry; 4) fluorescence spectrophotometry; 5) Titration; 6) Isotope dilution method.

The formation water in the Fengcheng Formation is rich in boron. In the northwestern margin of the Fengcheng area, the boron content ranges from 1.73 mg/L to 1,619.12 mg/L, with an average of 662.43 mg/L. The boron content of the Wuerhe area is 2.59 mg/L to 2,330.95 mg/L, with an average of 314.31 mg/L (Zhao et al., 2020), which is much higher than other areas in the basin. The $\delta^{11}B$ values of the Fengcheng Formation range from 0.33 to 2.13‰, with an average value of 1.08‰ (**Table 1**).

Boron isotope fractionation during water-rock interactions makes boron a good tracer of the hydrological cycle. In general, the $\delta^{11}B$ value of sedimentary rocks and magmatic rocks is about −40‰ ~ +30‰, the $\delta^{11}B$ value of continental crust is about −10 ± 2‰, and the $\delta^{11}B$ value of sea water is a constant +39.5‰ (Xiao et al., 2012). The $\delta^{11}B$ value of evaporate minerals varies greatly,

TABLE 2 | Selected data for fluid inclusion analysis of the Fengcheng Formation. The complete dataset is provided in **Supplementary Table S1**.

Well	Member	Depth/ m	Mineral type	Mineral texture	Inclusion type	Size/ μm	Homogenization temperature/°C	Freezing temperature/ °C
Fengcheng1	P_1f_1	3,970.50	calcite	growth zone	A	13	65	−4.0
Fengcheng1	P_1f_1	4,208.26	searlesite	growth zone	A	4	110	−6.2
Fengcheng1	P_1f_2	3,805.52	searlesite	growth zone	A	12	114	−19.2
Fengcheng1	P_1f_2	3,743.60	searlesite	long healed crack	A	7	110	−16.8
Fengcheng1	P_1f_3	4,228.35	calcite	long healed crack	A	6	170	−3.6
Fengcheng1	P_1f_3	4,228.35	searlesite	growth zone	A	6	100	−14.9
Fengnan2	P_1f_2	4,226.62	searlesite	growth zone	A	7	106	−19.2
Fengnan2	P_1f_2	4,226.62	searlesite	long healed crack	B	6	52	—
Fengnan2	P_1f_2	4,226.62	calcite	long healed crack	A	6	168	−4.8
Fengnan5	P_1f_2	4,130.20	searlesite	growth zone	A	8	106	−19.1
Fengnan5	P_1f_2	4,130.20	searlesite	growth zone	A	12	100	−16.6
Fengnan5	P_1f_2	4,130.20	searlesite	growth zone	A	10	100	−16.8

Note: A is liquid-rich gas-liquid two-phase saline inclusions, B is liquid-rich two-phase oil inclusions.

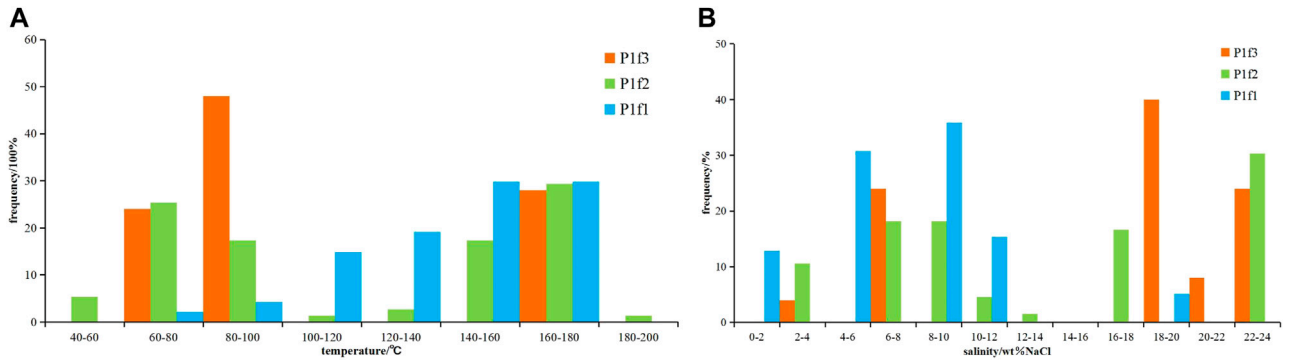

FIGURE 3 | Frequency diagrams for **(A)** homogenization temperature and **(B)** salinity of inclusions in the Fengcheng Formation.

and for non-marine evaporates $\delta^{11}B$ ranges from −32‰ to +8‰ (Xiao et al., 2012). This suggests that boron in the Fengcheng Formation originated from a deep hydrothermal source.

Fluid Inclusions

The inclusions were selected from calcites and searlesites. Under the microscope, the searlesite is colorless and transparent, coexisting with carbonate minerals, the interference color is gray to hoary, its particle size is 0.4–2.8 mm, and crystals are wedge-shaped or plate-like. Inclusions in searlesite occur as dispersed masses and veinlets. The fluid inclusions were mainly selected from primary inclusions in mineral growth zones and secondary inclusions in long healed cracks, that is, fluid captured during fracture healing after mineral growth. The types of inclusions included liquid-rich two-phase oil inclusions and liquid-rich two-phase saline inclusions. The homogenization temperature of saline inclusions in the growth zone was 65–114°C. In the long healed cracks, there were four oil inclusions with homogenization temperatures of 45–85°C, with an average of 60°C, while the freezing point temperatures could not be measured. The homogenization temperatures of saline inclusions in long healed cracks had a range of 110–175°C (**Table 2**). The homogenization temperatures of inclusions in each member of the Fengcheng Formation vary widely. The homogenization temperatures of Member I of the Fengcheng Formation are mainly from 100 to 180°C. The homogenization temperatures of Member II are in the range of 40–200°C, with two peaks at 60–100°C and 140–180°C. The homogenization temperatures of Member III are mainly at 60-100°C and 160–180°C (**Figure 3**). The peak homogenization temperature of inclusions decreases gradually from Member I to Member III, indicating that the fluids may be related to hydrothermal activity in the Early Permian. In a simple brine system the salinity (wt% NaCl eq) can be obtained by referring to the salinity freezing temperature conversion table in the standard method for determination of homogenization temperature and salinity of sedimentary rock inclusions (oil and gas industry standard of the people's Republic of China SY/T 6010-94). Salinities in the saline

TABLE 3 | Geochemistry of formation water of representative samples from wells in the Fengcheng Formation. The sodium chloride coefficient is [Na^+/Cl^-], the desulfurization coefficient is 100*SO_4^{2-}/Cl^-, and the metamorphic coefficient is [(Cl^--Na^+)/Mg^{2+}]. Data for all samples are in **Supplementary Table S2**.

Well	Member	Depth/m	Water type	Water level	PH	CO_3^{2-}/ mg/L	HCO_3^-/ mg/L	Cl^-/ mg/L	SO_4^{2-}/ mg/L	Ca^{2+} /Mg/L	Mg^{2+} /Mg/L	K^++Na^+ /Mg/L	Sodium chloride coefficient	Desulfurization coefficient	Metamorphic coefficient	Total dissolved solids/ mg/L
Fengcheng 1	P1f1	3,960.00 ~ 3,976.00	$NaHCO_3$		9.0	33135	30573	62772	3,378	98		79,154	2.35	–0.17	-4,266.14	209110
	P1f	4,206.00 ~ 4,232.00	$NaHCO_3$	I	9.7	34234	26107	22,059	3,269	20	7	51,922	0.88	–0.09		137618
Baiquan 1	P1f	4,724.00 ~ 4,734.00	$NaHCO_3$	I	8.9	11583	26264	97,111	8,390	0	0	85,801	0.86	–0.08		229149
	P1f	4,839.00 ~ 4,850.00	$NaHCO_3$	I	10.0	25542	2,140	113755	8,537	2	0	98,275	0.95	–0.24	42.53	248251
	P1f	4,096.00 ~ 4,108.00	$NaHCO_3$	I	8.5	231	7,496	13,493	2,601	102	15	12,855	1.54	–0.07	-629.80	36793
Wu 35	P1f	3,400.00 ~ 3,428.00	$NaHCO_3$	I	9.8	3,790	5,703	5,876	366	6	5	9,025	1.01	–0.05	-0.35	21919
Fengnan 8	P1f	4,256.00 ~ 4,286.00	$NaHCO_3$	I	9.2	6,162	13,611	24,795	1,118	42	728	25,051	1.01	–0.05	-0.44	71508
	P1f	4,256.00 ~ 4,286.00	$NaHCO_3$	I	9.2	6,436	13,298	24,790	1,157	73	735	25,110	0.92	–0.05	1,639.50	71599
Baiquan 5	P1f	3,966.00 ~ 3,971.00	$NaHCO_3$	I	9.0	6559	13,406	40,405	1,741	0	2	37,126	0.90	–0.04		99238
	P1f	3,966.00 ~ 3,971.00	$NaHCO_3$	I	8.8	4,591	11,872	33,543	1,168	0	0	30,316	2.60	–0.02		81490
Mahu15	P1f	3,962.00 ~ 3,972.00	$NaHCO_3$	I	9.2	55,750	36,047	29,052	591	0	0	75,453	2.62	–0.03		196893
	P1f	3,962.00 ~ 3,972.00	$NaHCO_3$	I	9.4	64,234	17253	28,520	938	0	0	74,694	2.35	–0.17	-4,266.14	185640
Fengnan4	P1f	4,635–4,648	$CaCl_2$	I	6.0	0.00	3,819.36	90196.07	823.96	25049.60	0.00	31604.07	0.54	–0.01		151493.06
Wu40	P1f	3,203–3,224	$CaCl_2$	I		0.00	8,786.38	48216.08	326.73	5,711.40	1883.72	24628.40	0.787	–0.01	12.52	85159.77
Wu351	P1f	3,144–3,156	$CaCl_2$	I	7.0	0.00	2,191.23	35207.81	194.26	1982.24	189.80	21127.34	0.93	–0.01	74.19	59797.07
Feng2	P1f	3,600–3,604	CaCl2	I		0.00	482.06	35275.74	574.45	4,809.60	243.06	17361.78	0.759	–0.02	73.70	58505.66
Bai73	P1f	3,710–3,726	MgCl2	I	6.5	0.00	674.27	30399.88	1,059.38	616.83	40.10	19699.50	0.999	–0.04	266.84	52152.83
Ke811	P1f	3,849–3,888	CaCl2	I		0.00	1,105.71	30674.47	65.21	1,418.23	122.89	18487.72	0.93	0.00	99.17	51874.22
Mahu7	P1f	4,012–4,030	CaCl2	I	6.5	0.00	2,693.54	23349.99	396.75	5,718.94	37.16	9,720.49	0.64	–0.02	366.78	41916.87
Ke821	P1f	3,464–3,476	CaCl2	I	7.0	0.00	2,559.67	22508.94	1,098.07	2,802.23	0.00	12878.16	0.88	–0.05		41847.07
K88	P1f	3,206–3,220	CaCl2	I	7.0	0.00	1,182.13	23633.14	1,545.03	2,975.79	89.73	12933.13	0.84	–0.07	119.25	41767.89
Bai25	P1f	3,284–3,346	CaCl2	I	11.0	723.14	122.55	18998.63	1,007.52	5,199.55	0.00	7,441.88	0.60	–0.06		33432.00
Baiwu3	P1f	3,154–3,180	CaCl2	I		132.00	146.44	18435.56	863.33	5,551.08	48.61	6066.71	0.507	–0.05	254.45	31170.51
197	P1f	2,660–2,675	Na2SO4	I		21.00	1,305.83	13916.87	1952.98	455.91	44.08	9,864.24	1.09	–0.16	91.94	26907.99
Bai25	P1f	3,022–3,032	CaCl2	I	7.0	0.00	612.76	15758.06	440.38	4,240.29	45.80	5,712.28	0.56	–0.03	219.34	26503.19
Ke811	P1f	3,791–3,823	CaCL2	I	6.0	0.00	1,164.48	13375.98	378.64	1,203.36	36.49	7,848.52	0.91	–0.03	151.48	24007.47
Ke204	P1f	4,323.5–4,334	CaCl2	I	6.0	0.00	1,516.47	12024.48	509.52	3,569.04	0.00	4,520.65	0.58	–0.04		22140.16
Ke201	P1f	4,143–4,158	CaCl2	I	6.0	0.00	1885.52	11695.59	146.52	3,603.99	0.00	4,232.23	0.56	–0.01		20621.09
Jianwu27	P1f	3,270–3,288	CaCl2	I		84.00	439.34	10742.26	1,077.31	1823.64	24.31	5,575.89	0.80	–0.11	212.52	19547.08
Bai257	P1f	2,949.5–2,956	CaCl2	I	8.5	63.81	843.55	10413.79	379.47	2,122.38	0.00	4,869.10	0.72	–0.04		18692.10
Xia40	P1f	4,831–4,886	Na2SO4	I	7		585	7,227	1,071	228	0	5,160	1.101	–0.17		13978
Bai261	P1f	3,150–3,168	Na2SO4	I	9.0	497.12	252.74	4,906.54	605.83	507.08	0.00	3,367.89	1.06	–0.14		10137.20
Jianwu42	P1f	2,898–2,916	Na2SO4	I		0.00	841.47	5,203.44	166.25	322.64	13.49	3,376.63	1.00	–0.03	135.42	9,503.18
Ke202	P1f	4,148–4,160	Na2SO4	I	8.6	361.86	184.28	4,338.38	870.88	65.33	33.06	3,163.65	1.13	–0.25	35.53	8,925.30
561	P1f	2,662–2,678	MgCl2	I		60.00	427.14	2,120.09	748.93	492.98	0.00	1,375.17	1.00	–0.55		5,011.74

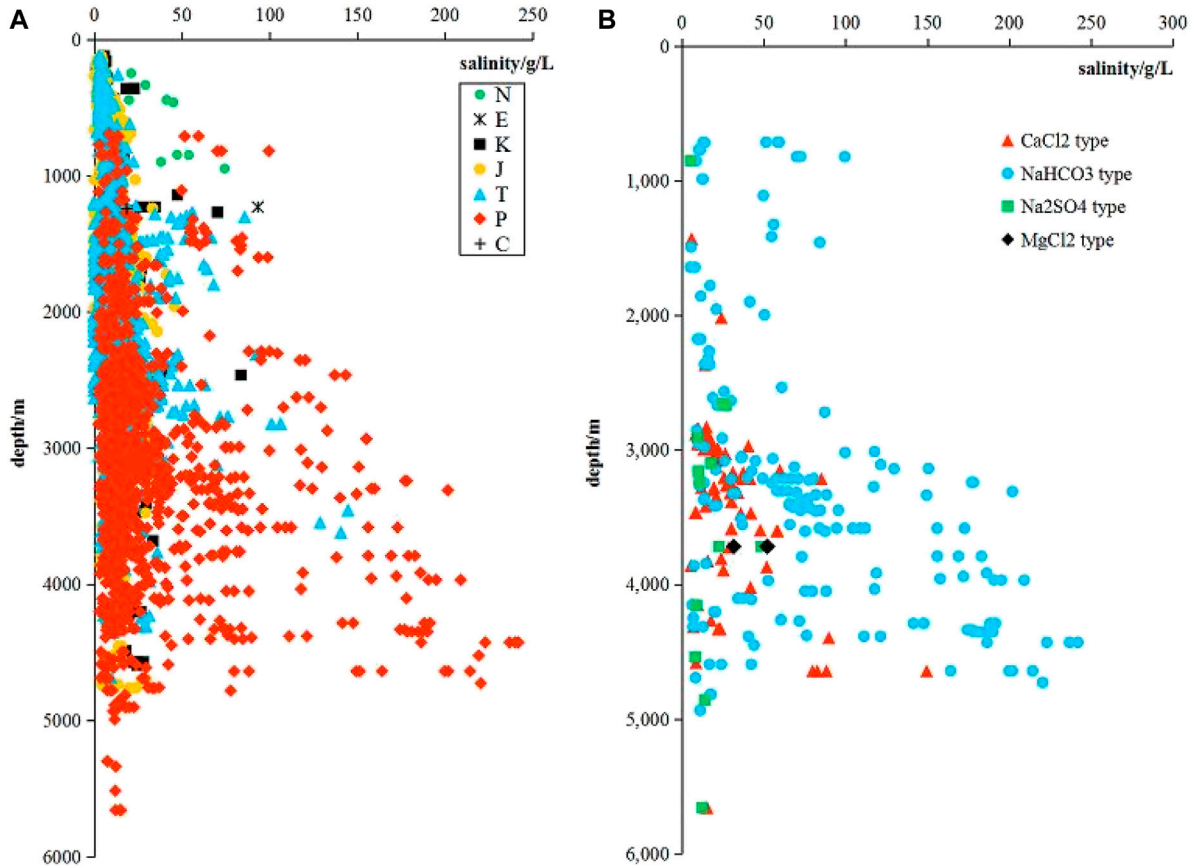

FIGURE 4 | Relationship between formation water mineralization degree and depth in **(A)** different horizons of the northwest margin of the Junggar Basin and **(B)** the Permian Fengcheng Formation. Abbreviations: C–Carboniferous, P–Permian, T–Triassic, J–Jurassic, K–Cretaceous, E–Eocene, N–Neogene.

inclusions ranged from 0 to 23.2 wt%. The freezing points of fluid inclusions in the Fengcheng Formation range from -1.1 to −19.5°C, with an average value of −11.1°C. The freezing point of inclusions in Member I is less than −8°C, and the salinity is generally less than 12%, with highest frequency at 4–6% and 8–10%. The freezing point of inclusions in Member II has a wide range, but the temperature ranges from -19.2 to −19.6°C. Most salinity values are between 22 and 24%, with secondary peaks at 6–10% and 16–18%. The freezing point and salinity of Member III are second only to Member II. The freezing point of inclusions in Member III ranges from −14.2 to −19.2°C, and the frequency of salinity values peaks at 18–20%, followed by smaller peaks at 6–8% and 22–24% (**Figure 3**). From the perspective of stratigraphy, salinity first increases and then decreases, showing a trend of low (Member I), high (Member II), low (Member III). A previous study also found that Member II has fluid inclusions with the highest salinity (Wang et al., 2003).

Geochemistry of Formation Water

All the formation water samples were collected from the wellhead or production pipeline. The water types and concentrations of major cations are listed in **Table 3**.

Overall, the formation water becomes more saline in the deeper and older horizons in the northwest margin of the Junggar basin, which indicates that the preservation conditions of deep formation water are better. The formation water of the Permian rocks is mainly $NaHCO_3$-type and $CaCl_2$-type, and the dissolved mineral content increases with depth. $CaCl_2$-type formation water is more common in deeper rocks, which suggests that the strata are well sealed and the formation water is continuously concentrated. This occurs because with increasing salinity, Na^+ in the water gradually exchanges with Ca^{2+} in the surrounding rock, which increases the Ca^{2+} in the solution and forms $CaCl_2$-type water. This process is called albitization. The formation water of the Fengcheng Formation is mainly $NaHCO_3$-type with high salinity, high HCO_3^- concentration, low Ca^{2+} concentration, low Mg^{2+} concentration and high pH, which is similar to the chemical composition of alkaline lake brine (**Table 3**). The salinity of formation water in the Fengcheng Formation is significantly higher than that of other Permian formations, with an average of 56.85 g/L, and nearly half of the samples are higher than that of modern seawater (35 g/L) (**Figure 4**). The correlation between salinity and Cl^- content of formation water in the Fengcheng Formation, especially at high salinity, is relatively poor. With

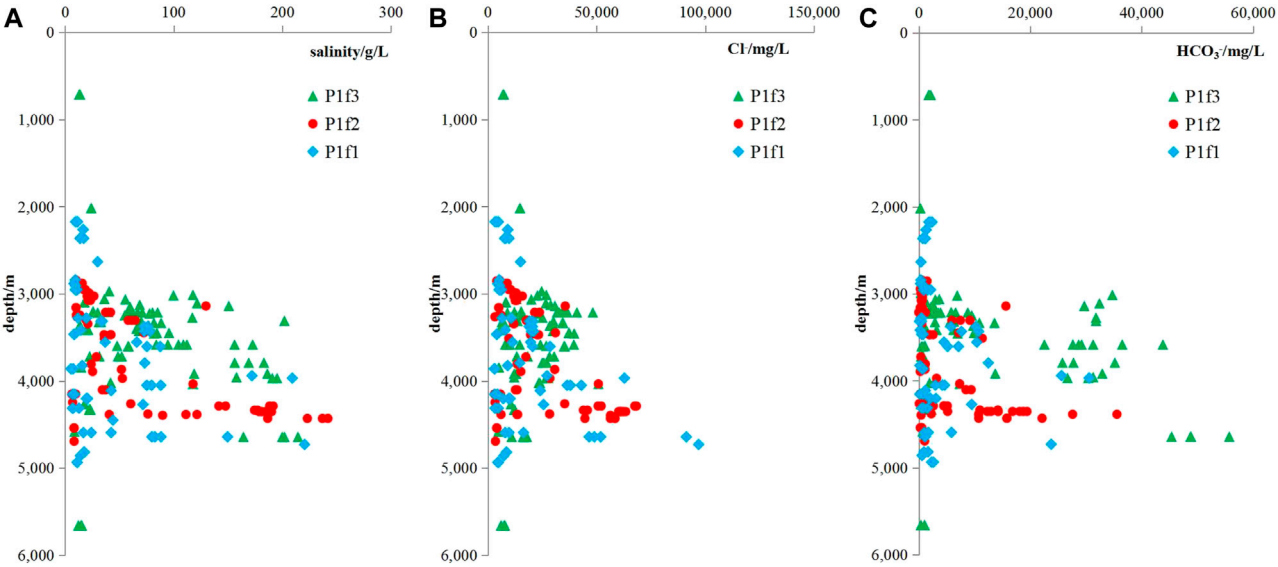

FIGURE 5 | Variation of **(A)** salinity, **(B)** Cl^-, and **(C)** HCO_3^- with depth in the Fengcheng Formation.

increasing salinity, Cl^- concentration does not strongly increase, but HCO_3^- concentration increases significant (**Table 3**; **Figure 5**). This shows that the high salinity of formation water in the Fengcheng Formation is the result of abnormally high HCO_3^- concentrations.

DISCUSSION

High HCO_3^- Source of the Fengcheng Formation

High-salinity $NaHCO_3$-type formation water is relatively rare in sedimentary basins. Some typical high-salinity $NaHCO_3$-type formation waters occur in the Huanghua Depression and Dongying Depression, and they are believed to be related to CO_2 from a mantle source or natural gas that migrated along large deep basement faults (Zhang Z et al., 2018). There are two deep source types for CO_2, i.e., mantle-magmatic origin and metamorphic origin (Zhao L et al., 2017). The high concentration of CO_2 in the deep layer results in increased concentrations of HCO_3^- and CO_3^{2-} in the water. Subsequently, some of the CO_3^{2-} combines with Ca^{2+} and Mg^{2+} in the water to precipitate $CaCO_3$ and $CaMg(CO_3)_2$, which greatly reduces the concentration of Ca^{2+} and Mg^{2+} content in water and makes the Na^+ and K^+ content dominant. The concentration of HCO_3^- in the study area is highest near the fault zone. The characteristics of carbon and oxygen isotopes and strontium isotopes of fluid inclusions indicate that the fluids near the fault zone have deep hydrothermal sources, and that volcanism contributes significantly to the source of CO_2. In addition, the boron concentration is abnormally high in the deep Permian and Carboniferous strata with high salinity. These sites are mainly distributed in the Wuerhe-Fengcheng area, so we speculate that these strata were affected by deep faults.

Another source of CO_2 is petroleum generation. In the Cenozoic strata in the Bohai Sea Area, large-scale petroleum generation and expulsion caused CO_2 gas to dissolve in water, which increases the concentration of HCO_3^- in aqueous solution and produces $NaHCO_3$-type water with high salinity (Zhao Z et al., 2017). Consequently, it is possible that in the process of migration and accumulation of light oil and gas generated by high and overmature petroleum source rocks in the northwest margin of the Junggar basin, the associated CO_2 entered into the formation water, and under certain conditions, high salinity $NaHCO_3$ formation water was formed. However, for reservoirs with high salinity $NaHCO_3$ formation water as bottom water, the density of crude oil is usually light (Chen et al., 2000). The petroleum-generating source rocks in the Fengcheng Formation in the Mahu Sag have mature organic matter, and a large amount of petroleum was generated and discharged, which may be another main reason for the high HCO_3^- content in the formation water.

Sealing of Deep Strata in the Fengcheng Formation

Previous studies have shown that, in general, reservoirs with greater degree of sealing have higher total salinity, Cl^- content and $K^+ + Na^+$ content, and lower HCO_3^- content (Zhao et al., 2020). The sealing effect is judged to be better when the sodium chloride coefficient is less than 0.85, the desulfurization coefficient is closer to 0, and the metamorphic coefficient [(Cl-Na)/Mg] is large and positive. The data for these coefficients (**Table 3**) indicate that the sealing of the Fengcheng Formation in wells Baiquan 1, Fengnan 8, and Fengcheng 1 is relatively good.

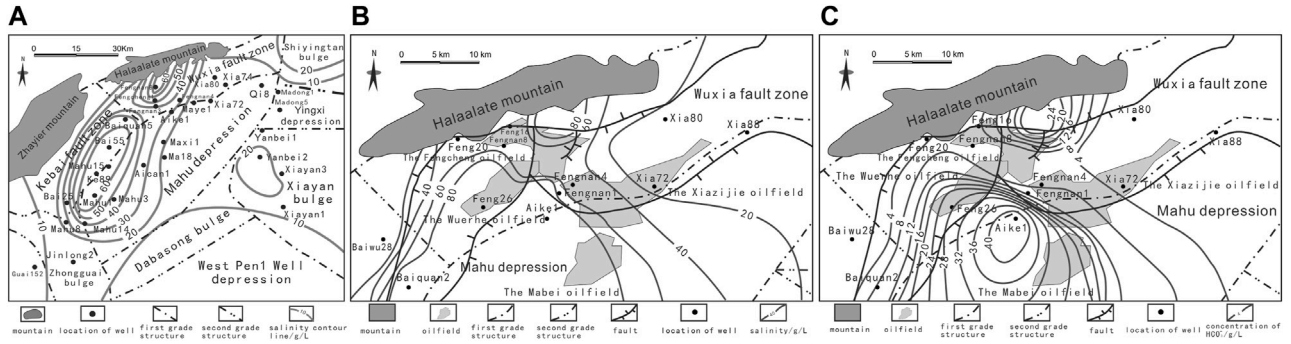

FIGURE 6 | Maps of dissolved mineral content. **(A)** Total dissolved minerals in the Permian system and **(B)** HCO_3^-concentration and **(C)** total dissolved minerals of the Fengcheng Formation in the northwestern margin of Junggar Basin.

The Permian strata in Junggar basin are very deeply buried (generally between 3,000 and 5,000 m), the formation is relatively closed, and the formation water salinity is high. The average formation water salinity of the Permian Fengcheng Formation in the Mahu area exceeds 50 g/L, and the formation water salinity is highest at depths of 4,424–4,437 m in well Mahu 16, with an average value of 241.87 g/L in this interval. In some areas, due to seepage of fresh water along the fault, formation water becomes less saline and changes to Na_2SO_4- type. The decrease of salinity and changes of water type in this area suggest that the preservation conditions of oil and gas have worsened, which could mean that the oil has been thickened. For example, in wells Ke 78 and Ke 79, the salinity of the Permian Fengcheng Formation water is 6.58 g/L (3,347–3,355 m) and 4.94 g/L (3,423–3,436 m), and the crude oil density is 0.9495 g/cm^3 and 0.9362 g/cm^3, respectively. Relatively shallow wells near the margin of basin are affected by meteoric water, and the conditions for oil and gas preservation are poor. For example, in well Baiwu 28 (1,410–1,448 m), the formation water salinity is only 5.90 g/L and the crude oil density is 0.9019 g/cm^3. The mineralization of the high part of the structure is affected by the infiltration of atmospheric water, and the influence of meteoric water weakens at greater depths. The infiltration of atmospheric water leads to desalination of formation water, lower dissolved mineral content, oxidation and biodegradation of crude oil, and thickening of oil, which is not conducive to the accumulation and preservation of oil and gas. Heavy oil in the northwest margin of Junggar basin is mostly distributed at depths of less than 1,000 m (**Figure 6**), which is basically consistent with the distribution of formation water with low salinity and low chloride concentration.

On the map view, high salinity $NaHCO_3$ water is dominant in the Baikouquan-Wuerhe-Fengcheng area around the Mahu Sag. The dissolved mineral content of formation water in these areas reaches 200 g/L and higher, and is mainly concentrated in the Fengcheng Formation (**Figure 6**). Due to the infiltration of meteoric water at the margin of the basin, the formation water types are mostly $NaHCO_3$ or Na_2SO_4 with low salinity, whereas the other areas are mostly $CaCl_2$ water, indicating that the overall condition of oil and gas preservation is good (**Figure 5**).

The overall hydrodynamic state of the Permian is overpressure. The hydraulic head gradually decreases from the Mahu Sag to the northwest margin. The hydraulic head gradient near Wuerhe in the north section is relatively high, and the hydrodynamic effect is relatively strong, which is not conducive to petroleum accumulation and preservation. The Baikouquan, Karamay and Che Guai areas are low pressure potential areas, and the gradient of hydraulic head becomes more gradual, which is favorable for oil and gas accumulation (Jian et al., 2020).

Sedimentary Environment and Significance of the Fengcheng Formation

The carbon, oxygen, strontium, and boron isotopes show that the Fengcheng Formation in the Mahu Depression may be affected by deep hydrothermal fluids. Previous studies suggested that the Fengcheng Formation was deposited in an alkaline lake characterized by a closed environment, dry climate, and intense evaporation (Zhang Y et al., 2018; Zhao et al., 2020). Both volcanism and petroleum generation and expulsion from source rocks can provide abundant CO_2, which dissolves in the water and results in a high concentration of HCO_3^- and high pH and alkalinity. The areas of high salinity and HCO_3^- in formation water in the Fengcheng Formation are mainly in the southwestern slope area (**Figure 6**). Fluid inclusion salinity data also show that high salinities occur in wells Fengnan 7, Feng 26, Feng 5, and Aike1, and the distribution is generally consistent with the high salinity area. In addition, alkaline minerals in these areas are also prevalent. Therefore, the highest alkalinity in the study area appears to occur in the southwest slope of the Mahu Depression.

The evolution of alkaline lakes frequently includes a complete sequence: alkali-preparation, primary alkali, strong alkali formation, weak alkali formation and termination phase, and this evolutionary sequence is well recorded in the Fengcheng Formation (Zhang Z et al., 2018). The different geochemical characteristics of formation water in each member of the Fengcheng Formation can reflect its evolutionary stages. Data from the chemical analysis of formation water and fluid inclusion analysis show that the salinity is low in Member I, gradually

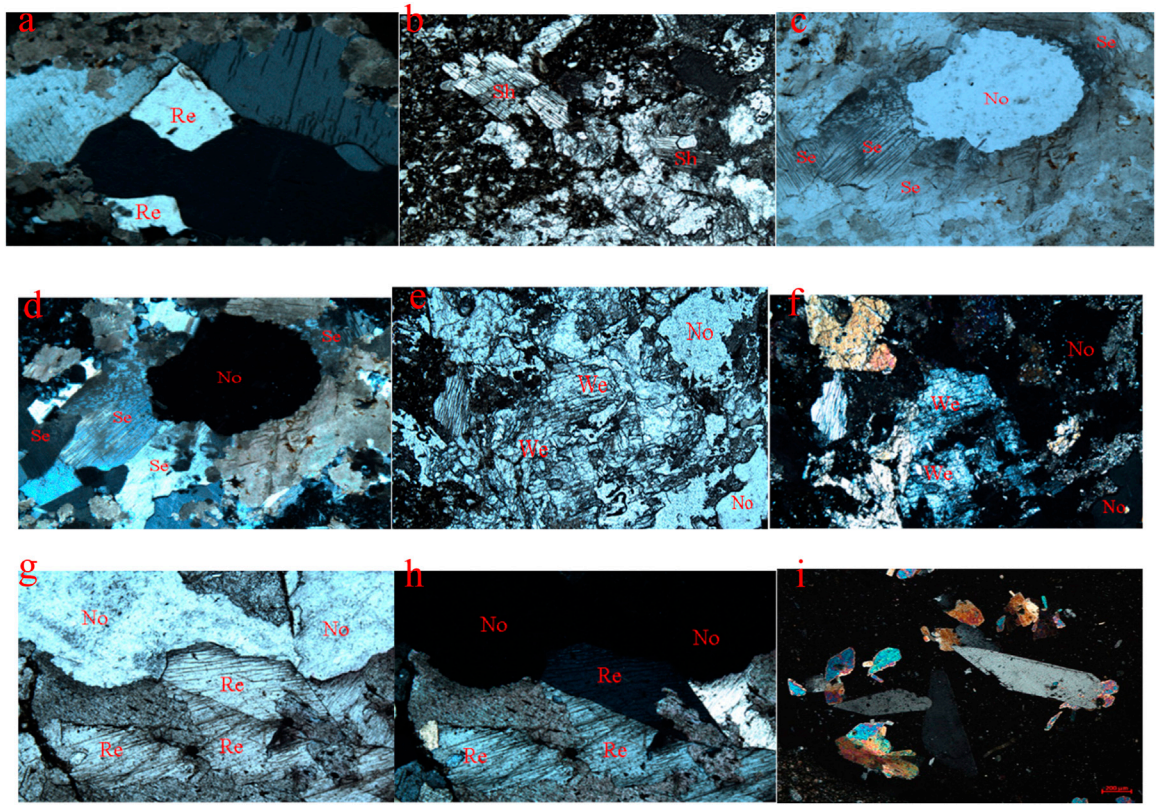

FIGURE 7 | Alkaline minerals of the Permian Fengcheng Formation, Mahu Depression. **(A)** Fengnan 1, P_1f^2, 4,192.65 m, cross-polarized light x10; **(B)** Fengnan7, P1f2, 4,595.3 m, plane-polarized light x5; **(C)** Feng 8, P1f2, 3,091.78 m, plane-polarized light x10; **(D)** Feng 8, P1f2, 3,091.78 m, cross-polarized light x10; **(E)** Fengnan 7, P1f2, 4,595.3 m, plane-polarized light x5; **(F)** Fengnan, P1f2, 4,595.3 m, cross-polarized light x5; **(G)** Aike1, P1f1, 5,666.4 m, plane-polarized light x5; **(H)** Aike 1, P1f1, 5,666.4 m, cross-polarized light x5; **(I)** Fengcheng 1, P_1f^1, 4,273.75 m, cross-polarized light. (Re: Reedmergnerite, No: Northupite, Se: Searlesite, Sh: Shortite, We: Wegscheiderite).

increases in Member II, then decreases in Member III. Together with salinity, the Cl^- concentration increases in Member II, and the HCO_3^- concentration is highest in Member III (**Figure 5**).

The mineralogy of the Fengcheng Formation also provides clues about the depositional environment. By using microscopic observation, we found abundant reedmergnerite ($NaBSi_3O_8$) and shortite ($Na_2Ca_2(CO_3)_3$), especially in Member II of the Fengcheng Formation. In recent years, some studies (Jagniecki et al., 2013; Guo et al., 2021) have suggested that the temperature of formation of shortite is greater than 52 ± 2°C, which cannot occur in a subaerial alkaline evaporative lake environment. Most of the shortite in the study area occurs in reticular veins. There are two possible scenarios for the formation of shortite: 1) the hydrothermal fluid from the deep crust mixes with the formation water enriched in CO_3^{2-} and Ca^{2+}, resulting in the precipitation of gaylussite in the fracture, which gradually dehydrates to form shortite as temperature and pressure increase along with burial; 2) a pulse of hydrothermal fluid releases pressure along a fault under intense tectonic and volcanic action, which makes the recently consolidated fine sediment rapidly burst into fragments. The mixing of the deep hydrothermal fluid and lake water at the bottom of the lake leads to changes in pressure and concentration. The first mineral to precipitate in the fissure network is gaylussite, and then the increase of formation temperature and pressure in the later deep burial process leads to the formation of shortite. This indicates that the occurrence in the study area of the hydrothermal sedimentary minerals reedmergnerite and shortite may be related to magmatic activity. This scenario is further supported by the location of reedmergnerite and shortite mostly in wells near faults and the occurrence of volcanic rocks in these drill cores (**Figure 7**).

The alkaline minerals of the Fengcheng Formation mainly occur in the east and southeast of the Wuerhe area in the Mahu Depression. The highest concentrations of alkaline minerals are in Member II of the Fengcheng Formation. It can be inferred that Member I represents the initial stage of alkaline lake formation, corresponding to a high lake level and relatively low salinity. Member II represents the strong alkali forming stage, corresponding to falling lake levels. During this stage, the lake level dropped, salinity increased, and alkaline minerals were precipitated. Member III represents the expansion of the

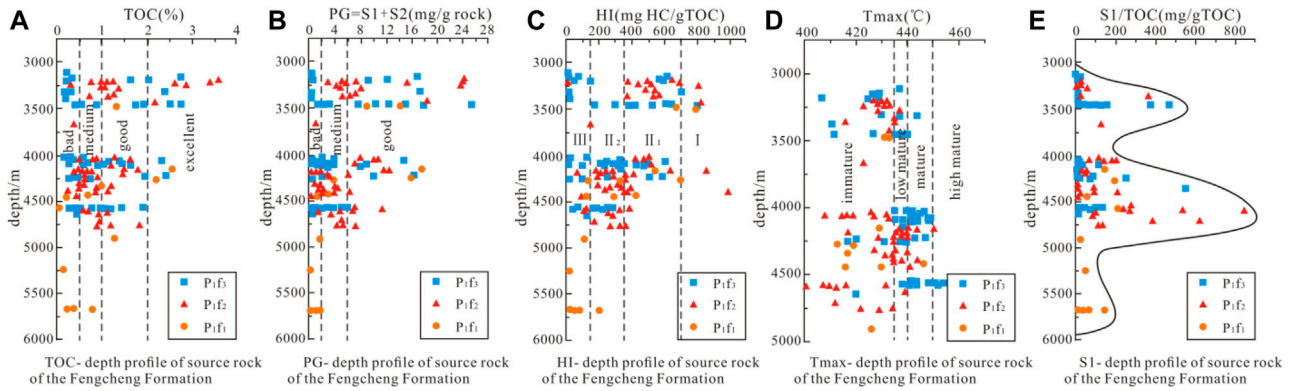

FIGURE 8 | Organic geochemical profiles of source rocks in the Fengcheng Formation in the Mahu Sag (Cao et al., 2015. **(A)** TOC-depth profile of source rock of the Fengcheng Formation. **(B)** PG-depth profile of source rock of the Fengcheng Formation. **(C)** HI-depth profile of source rock of the Fengcheng Formation. **(D)** Tmax-depth profile of source rock of the Fengcheng Formation. **(E)** SI-depth profile of source rock of the Fengcheng Formation).

alkaline lake, corresponding to the early stage of lacustrine transgression, and both the salinity and the concentration of alkaline minerals decreased gradually. Therefore, Member II was deposited in the most alkaline stage of the lake's evolution.

In map view, the area of greatest alkaline mineral deposition coincides with the area of highest formation water salinity, indicating that the alkaline lake was formed in a semi closed basin (Zhang Z et al., 2018). The distribution of alkaline lake source rocks in the Fengcheng Formation in the Mahu Sag is uniform, and the cumulative thickness is more than 200 m, which indicates a good potential for petroleum generation. The addition of exhalative hydrothermal solution and volcanic materials in the lake basin likely promoted the periodic growth of bacteria and algae. Petrographic examination performed in another study shows that laminate structures formed by microorganisms and layered algae are interbedded in striate form with inorganic minerals in the source rocks of Fengcheng Formation (Cao et al., 2019).

The alkaline lake source rocks have typical characteristics of high-quality source rocks. The Fengcheng Formation has high content of organic matter that is mainly Type I-II_1 and sapropel type (**Figure 8C**). This type of organic matter is oil-generative, which is consistent with the greater quantity of oil than gas found in the study area. Organic geochemical analysis of Fengcheng Formation source rocks shows that the total organic carbon content is good to excellent (**Figure 8A**, **Figure 8B**), which, when combined with the oil-generative organic matter type, indicates a good oil generation potential. This is consistent with the discovery of large oil and gas reservoirs in the study area. Most of the analyzed samples have low maturity (**Figure 8D**), but the maturity of source rocks in the sag is relatively high. In general, the Fengcheng Formation source rocks have high total organic carbon concentrations, are mainly oil-generative, and within the sag area they are mature to highly mature. These properties indicate good petroleum generation potential and the potential for the formation of large oil and gas fields (Cao et al., 2015).

Hydrothermal activities increase the maturity of kerogen and result in an abnormal petroleum generation evolution curve and lengthening of the oil generation window. Early alkaline minerals promote the condensation dehydrogenation of kerogen and increase the yield of liquid petroleum (Wang et al., 2015). Alkaline minerals are lipophilic (Hu et al., 2015), and a large amount of crude oil accumulates to form overpressure, which can delay petroleum generation. In fact, due to the protection and inhibition of organic matter by environmental factors, the measured organic geochemical parameters of alkaline lacustrine source rocks are lower, so the actual petroleum generation potential of the Fengcheng Formation may be far better than that seen from geochemical indicators. This may also be the reason why the exploration results of Fengcheng Formation petroleum system are much better than the results of resource evaluation based on the indicators of source rocks.

CONCLUSION

(1) The Fengcheng formation is characterized by $NaHCO_3$-type formation water with high salinity, high HCO_3^- concentration, low Ca^{2+} concentration, low Mg^{2+} concentration and high pH, indicating that the formation sealing is good. In the shallow wells near the edge of the basin in which meteoric water has infiltrated along the fault, the amount of dissolved minerals decreases and Na_2SO_4-type water evolves, so the oil and gas preservation conditions are relatively poor.

(2) The fluid geochemistry and distribution of alkaline minerals in the strata dominated by deep fine-grained mixed sediments, which indicates that the Fengcheng Formation was deposited in an alkaline lake environment. The isotopic compositions of carbon, oxygen, strontium and boron all indicate that the deposition of the Fengcheng Formation in the Mahu Sag may be affected by deep hydrothermal activity. The paleosalinity is low in Member I, high in Member II, and low in Member III, corresponding to the stages of initial alkaline lake development, high alkaline mineral concentrations, and decreasing alkalinity.

(3) The spatial coincidence of alkaline minerals, high salinity of formation water and source rocks indicates that the alkaline lake environment can form high-quality source rocks with good petroleum generation potential.

DATA AVAILABILITY STATEMENT

The original contributions presented in the study are included in the article/**Supplementary Material**, further inquiries can be directed to the corresponding authors.

AUTHOR CONTRIBUTIONS

JW: Work concept or design, Draft paper, Make important revisions to the paper, Approve final paper for publication LZ: Work concept or design JL: Work concept or design, Data collection XZ: Make important revisions to the paper XL: Data collection RZ: Data collection YW: Data collection ZR: Data collection JD: Approve final paper for publication.

FUNDING

This study was funded by the National Science and Technology Major Project (grant No. 2017ZX05008-004-008) of China.

SUPPLEMENTARY MATERIAL

The Supplementary Material for this article can be found online at: https://www.frontiersin.org/articles/10.3389/feart.2021.774501/full#supplementary-material

REFERENCES

Cao, J., Lei, D., Li, Y., Tang, Y. A. B., and Chang, Q. (2015). High-quality Hydrocarbon Source Rocks in Ancient Alkaline lake: Fengcheng Formation of Lower Permian, Junggar Basin. *Acta Petrolei Sinica* 36 (7), 781–790. doi:10.7623/syxb201507002

Cao, J., Hu, W., Yao, S., Zhang, Y., Wang, X., Zhang, Y, et al. (2007). Carbon, Oxygen and Strontium Isotope Composition of Calcite Veins in the Carboniferous to Permian Source Sequences of the Junggar Basin: Implications on Petroleum Fluid Migration. *Acta Sedimentologica Sinica* 25 (5), 722–729. doi:10.3969/j.issn.1000-0550.2007.05.010

Cao, J., Xia, L., Wang, T., Zhi, D., Li, W., et al. (2019). An Alkaline lake in the Late Paleozoic Ice Age (LPIA): A Review and New Insights into Paleoenvironment and Hydrocarbon Potential. *Earth-Science Rev.* 202, 103091. doi:10.1016/j.earscirev.2020.103091

Chang, H., Zheng, R., Guo, C., and Wen, H. (2016). Geochemical Characteristics of Rare Earth Elements in the Effluents of the Fengcheng Formation in the Northwestern Margin of Junggar Basin. *Geol. Rev.* 62 (3), 550–564. CNKI: SUN:DZLP.0.2016-03-003

Chen, J., Cha, M., and Zhou, Y. (2000). Chemical Characteristics of Formation Water in Relation with Oil/gas in the Northwestern Parts of Junggar Basin. *Geology. Geochem.* 28 (3), 54–58. doi:10.3969/j.issn.1672-9250.2000.03.006

Feng, J., Hu, K., Cao, J., Chen, Y., Wang, L., Zhang, Y., et al. (2011). Terrigenous Clastic Carbonate Mixers and Their Hydrocarbon Geological Significance. *Geol. J. China Universities* 17 (2), 297–307. doi:10.3969/j.issn.1006-7493.2011.02.015

Garven, G. (1989). The Geology of Fluid Flow: Fluid Flow in Sedimentary Basins and Aquifers. *Science* 243 (3), 677. doi:10.1126/science.243.4891.677

Gieskes, J. M., Elderfield, H., and Palmer, M. R. (1986). Strontium and its Isotopic Composition in Interstitial Waters of marine Carbonate Sediments. *Earth Planet. Sci. Lett.* 77, 229–235. doi:10.1016/0012-821x(86)90163-9

Guo, P., Wen, H., Li, C., Jin, J., and Lei, H. (2021). Origin and Enrichment of Borates in a Late Paleozoic Alkaline lake-playa deposit, Junggar Basin, NW China. *Ore Geology. Rev.* 138, 104389. doi:10.1016/j.oregeorev.2021.104389

He, D., Zhang, L., Wu, S., Li, D., and Zhen, Y. (2018). Tectonic Evolution Stages and Features of the Junggar Basin. *Oil Gas Geology.* 39, 846–861. doi:10.11743/ogg20180501

Hu, Q.-H., Liu, X.-G., Gao, Z.-Y., Liu, S.-G., Zhou, W., and Hu, W.-X. (2015). Pore Structure and Tracer Migration Behavior of Typical American and Chinese Shales. *Pet. Sci.* 12, 651–663. doi:10.1007/s12182-015-0051-8

Jagniecki, E. A., Jenkins, D. M., Lowenstein, T. K., and Carroll, A. R. (2013). Experimental Study of Shortite (Na2Ca2(CO3)3) Formation and Application to the Burial History of the Wilkins Peak Member, Green River Basin, Wyoming, USA. *Geochimica et Cosmochimica Acta* 115, 31–45. doi:10.1016/j.gca.2013.04.005

Jian, W., Lu, Z., Jin, L., Yong, W., Yang, Y., Baozhen, Z., et al. (2020). Characteristics and Origin of the Fengcheng Formation Water in Mahu Depression and its Significance to Hydrocarbon Migration and Accumulation. *IOP Conf. Series: Earth Environ. Sci.* 600, 012033. doi:10.1088/1755-1315/600/1/012033

Jiang, Y., Wen, H., Qi, L., Zhang, X., and Li, Y. (2012). Salt Minerals and Genetic Analysis of Fengcheng Formation, Permian, Wuerhe Area, Junggar Basin. *J. Mineralogy Petrol.* 32 (2), 105–114. doi:10.3969/j.issn.1001-6872.2012.02.014

Jin, A., Lou, Z., and Zhu, R. (2006). Characteristics of Groundwater Chemical Distribution in Northwestern Margin of Junggar Basin. *Nat. gas industry* 26 (11), 14–17. doi:10.3321/j.issn:1000-0976.2006.11.005

Keith, M. L., and Weber, J. N. (1964). Carbon and Oxygen Isotopic Composition of Selected Limestones and Fossils. *Geochimica et Cosmochimica Acta* 28, 1787–1816. doi:10.1016/0016-7037(64)90022-5

Kuang, L., Tang, Y., and Lei, D. (2012). Formation Conditions and Exploration Potential of the Permian saline Lacustrine Cloud Rock Tight Oil in Junggar Basin. *Pet. Exploration Develop.* 39 (6), 657–667. doi:10.1016/s1876-3804(12)60095-0

Liu, D., Sun, X., Li, Z., Tang, N., Tan, Y., and Liu, B. (2006). Carbon and Oxygen Isotope Analysis of Ordovician Dolomite in Ordos Basin. *Pet. Exp. Geology.* 28 (2), 155–161. doi:10.3969/j.issn.1001-6112.2006.02.012

Liu, Y., Yuan, H., Gao, Y., Zhao, Y., and Xu, G. (2017). Genesis Mechanism and Petroleum Geological Significance of Carboniferous - Permian Fissure Filling Calc in Haashan Area Junggar Basin. *Acta Geologica Sinica* 91 (11), 2573–2583. doi:10.1111/1755-6724.13367

Lou, Z., Jin, A., and Fu, X. (2006). Hydrogeochemistry of Marine Subsurface and Evaluation of Hydrocarbon Preservation Conditions. *J. Zhejiang Univ. (Engineering Sci. edition* 40 (3), 501–505. doi:10.3785/j.issn.1008-973X.2006.03.029

Lou, Z., Jin, A., and Tian, W. (2005). On the Dynamic Field of Groundwater and Hydrocarbon Migration and Accumulation in continental Sedimentary basin. *Geol. Sci.* 40 (3), 305–318. doi:10.3321/j.issn:0563-5020.2005.03.001

Lou, Z., Zhu, R., and Jin, A. (2009). The Relationship between Groundwater and Hydrocarbon Accumulation and Preservation in Sedimentary basin. *Acta Geologica Sinica* 83 (8), 1188–1194.

Mello, M. R., and Maxwell, J. R. (1990). "Organic Geochemical and Biological Marker Characterization of Source Rocks and Oils Derived from Lacustrine Environments in the Brazilian continental Margin: Chapter 5 of Lacustrine basin Exploration," in *Case Studies and Modem Analogs*. AAPG Bulletin. Editor B. J. Katz, 77–97. doi:10.1306/d9cb5e67-1715-11d7-8645000102c1865d

Meng, W., Li, Y., Fu, G., and Li, J. (2018). Relationship between Chemical Characteristics of Formation Water and Natural Gas Accumulation within Shan 2 Member of Shanxi Formation in North Yulin Gas Field. *Northwest. Geology.* 51 (2), 203–208. doi:10.19751/j.cnki.61-1149/p.2018.02.027

Palmer, M. R., and Edmond, J. M. (1989). The Strontium Isotope Budget of the Modern Ocean. *Earth Planet. Sci. Lett.* 92, 11–26. doi:10.1016/0012-821x(89)90017-4

Qin, Z., Chen, L., Li, Y., Wang, T., and Cao, J. (2016). The Paleosedimentary Background of Jiancheng Formation, Lower Permian, Mahu Sag, Junggar Basin. *Xinjiang Pet. Geology.* 37 (1), 1–6. doi:10.7657/XJPG20160101

Si, Y. (2019). *Study on the Relationship between Formation Water and Reservoir in Chang 8 and Chang 9 Low Permeability sandstone Reservoirs in Jiyuan Area, Ordos Basin*. PhD Dissertation. Xi'an, China: Northwest University.

Wang, M., Zhang, Z., Zhou, C., Yuan, X., Lin, M., Liu, Y., et al. (2018). Characteristics and Genesis of Alkali-lake Rocks in the Fengcheng Formation of Lower Permian in Mahu Sag Junggar Basin. *J. Palaeogeogr.* 20 (1), 147–162. doi:10.7605/gdlxb.2018.01.010

Wang, T., Yang, S., Duan, S., Chen, H., Liu, H., and Cao, J. (2015). Multi-Stage Primary and Secondary Hydrocarbon Migration and Accumulation in Lacustrine Jurassic Petroleum Systems in the Northern Qaidam Basin, NW China. *Mar. Pet. Geology.* 62, 90–101. doi:10.1016/j.marpetgeo.2015.01.015

Wang, X., Wang, T., and Cao, J. (2018). Basic Characteristics of Hydrocarbon Source Rocks and Their High Efficiency Hydrocarbon Generation in Fengcheng Formation, Mahu Depression. *Xinjiang Pet. Geology.* 39 (1), 9–15. doi:10.7657/XJPG20180102

Wang, Z., Zhang, S., Tian, Y., Liu, G., Li, Z., and Xiang, S. (2003). The Genesis of Stratigraphic Activated Water in Junggar Basin and its Relationship with Oil and Gas Reservoirs. *Xinjiang Pet. Geology.* 24 (02), 112–114.

Wei, Y., Guo, P., Jin, J., Jiang, Y., Wang, J., Lei, H., et al. (2021). Origin of Chert in Volcanic Alkali lake Sedimentary Rocks: a Case Study of Fengcheng Formation of Lower Permian in Junggar Basin. *J. sedimentation* 41 (2), 83–98. doi:10.19719/j.cnki.1001-6872.2021.02.08

Xia, L., Cao, J., Xu, T., Wang, T., Zhang, Y., and Bian, L. (2017). The Biodevelopment Characteristics of Salt Lake and its Hydrocarbon Source Significance. *Geol. Rev.* 63 (06), 123–136. doi:10.16509/j.georeview.2017.06.010

Xian, B., Niu, H., Zhu, X., Dong, G., Zhu, S., and An, S. (2013). Lithology Lithofacies of Lower Permian Volcanic Rocks and Their Relationship with Reservoirs in the Northwestern Margin of Junggar Basin. *Geol. J. China Universities* 19 (1), 46–55. doi:10.16108/j.issn1006-7493.2013.01.005

Xiao, J., He, M., Xiao, Y., and Jin, Z. (2012). Advances in Research on boron Isotope Geochemistry. *Mar. Geol. frontier* 28 (9), 20–29. doi:10.16028/j.1009-2722.2012.09.010

Yang, J., Yi, C., Du, Y., Zhang, Z., and Yan, J. (2014). The Geochemical Characteristics of Paleogene Alkali-Bearing Rocks in Biyang Depression Are Indicative of Alkali-Forming. Chinese Science:. *Earth Sci.* 44 (10), 2172. doi:10.1360/zd-2014-44-10-2172

Zeng, G., Wang, F., Zheng, J., and Cheng, Z. (2002). Pyroxene in Basement Volcanic Rocks of Junggar Basin and its Tracer to Basement Properties of the basin. *Earth Sci. - J. China Univ. Geosciences* 27 (1), 13–18. doi:10.3321/j.issn:1000-2383.2002.01.003

Zhang, H., Xu, T., Xie, Y., Zhang, H., Fan, S., and Chen, C. (2021). Hydrochemical Characteristics of Ahe Formation in Eastern Kuqa Depression, and its Hydrocarbon Response. *Geology. China* 11.

Zhang, Y., Li, W., and Tang, W. (2018). The Tectonic Background and Forming Environment of Hydrocarbon Source Rocks in Fengcheng Formation in Mahu Depression. *Xinjiang Pet. Geology.* 39 (1), 48–54. doi:10.7657/XJPG20180106

Zhang, Z., Yuan, X., and Wang, M. (2018). Alkaline-lacustrine Deposition and Paleoenvironmental Evolution in Permian Fengcheng Formation at the Mahu Sag, Junggar Basin, NW China. *Pet. Exploration Develop.* 45 (6), 972–984. doi:10.1016/s1876-3804(18)30107-1

Zhao, L., Jia, F., Cao, J., Liu, H., Bian, X., and Gao, J. (2017). The Fluid Movement Process in the Fault and its Influence on Fault Opening and Closing in the Northwest of Junggar Basin. *Pet. Exp. Geology.* 39 (4), 461–466. doi:10.11781/sysydz201704461

Zhao, Y., Guo, P., Lu, Z., Zhen, R., Chang, H., and Wang, G. (2020). Development Characteristics and Enrichment Genesis of Sodalite in Fengcheng Formation of Lower Permian in Junggar Basin. *J. Sedimentation* 38 (5), 966–979. doi:10.14027/j.issn.1000-0550.2019.110

Zhao, Z., Guan, D., Wei, A., Liu, P., and Fu, L. (2017). Chemical Characteristics and Main Controlling Factors of Formation Water in Cenozoic in Bohai Sea (In Chinese with English Abstract). *Nat. Gas Geosci.* 28 (9), 1396–1405. doi:10.11764/j.issn.1672-1926.2017.08.016

Zhi, D., Cao, J., Xiang, B., Cao, J., and Wang, T. (2016). A New Understanding of Hydrocarbon Generation Mechanism and Resource Quantity of Hydrocarbon Source Rocks in Fengcheng Formation in Mahu Depression. *Xinjiang Pet. Geology.* 37 (5), 499–506. doi:10.7657/XJPG20160501

Conflict of Interest: The authors declare that the research was conducted in the absence of any commercial or financial relationships that could be construed as a potential conflict of interest.